Effect of Temperature and Span Series Surfactant on the Structure of Polysulfone Membranes

Hui-An Tsai,[1,2] Ruoh-Chyu Ruaan,[1] Da-Ming Wang,[3] Juin-Yih Lai[1]

[1] *R&D Center for Membrane Technology, Department of Chemical Engineering, Chung Yuan University, Chung Li, 32023, Taiwan, Republic of China*
[2] *Department of Textile Engineering, Nanya Institute of Technology, Chung Li, 32034, Taiwan, Republic of China*
[3] *Department of Chemical Engineering, National Taiwan University, Taipei 10617, Taiwan, Republic of China*

Received 21 May 2001; accepted 9 January 2002

ABSTRACT: A macrovoid structure was found in polysulfone membranes formed by the wet-inversion method using *N*-methylpyrrolidinone (NMP) and water as the solvent/nonsolvent pair. The addition of Span series surfactants in the casting solution was found to inhibit the macrovoid formation. Sorbitan monooleate (Span-80) was more effective in inhibiting macrovoids than was sorbitan monolaurate (Span-20). The phenomenon of macrovoid suppression became more prominent at higher temperature. The cloud-point shift might account for the temperature effect. But there was no simple explanation for the effect caused by Span-80. The cloud-point position, the demixing rate, and the viscosity of the casting solution were measured. None of them could explain the effect of macrovoid inhibition by the addition of Span-80. However, the penetration test indicated that the penetration of a nonsolvent into a surfactant-free casting solution was caused by a convective flow, but that into Span-80 was through diffusion. It was found that the retardation of nonsolvent penetration was the major cause of macrovoid inhibition. © 2002 Wiley Periodicals, Inc. J Appl Polym Sci 86: 166–173, 2002

Key words: membranes; surfactants; phase diagrams

INTRODUCTION

The wet-inversion method has been widely adopted to prepare asymmetric membranes. It is generally accepted that the membrane structure is affected by both the system thermodynamics and the process kinetics. The system thermodynamics is often demonstrated by a ternary phase diagram. The binodal curve of liquid–liquid phase separation was considered an important factor affecting the membrane structure. The cloud-point curve was usually measured to represent the binodal curve. Mulder,[1] Altena and Smolders,[2] Wijmans et al.,[3] and Lau et al.[4] believed that liquid–liquid phase separation could occur more easily in a system with a wider demixing gap. The solvent–nonsolvent exchange rate was one of the kinetics factors attracting the most attention: It determined the path on the phase diagram during membrane formation. Smolders et al.,[5] Tsay and McHugh,[6] Radovanoric et al.,[7,8] and Reuvers[9] developed several mass-transfer models to predict the composition when phase separation first occurred and the demixing time from encountering a nonsolvent to phase separation. Reuvers[9] developed a light-transmission experiment to measure the demixing rate. Two distinct types of a light-transmission pattern were observed: instantaneous demixing and delayed demixing. It was found that the system of instantaneous demixing often led to a fingerlike membrane structure and delayed demixing often lead to spongelike structure.

The membrane structure made by the wet-inversion method was not only affected by the types of polymer/solvent pairs, the polymer concentration of the casting solution, and the type of nonsolvent used, but was also affected by the additives added to the casting solution or to the coagulant. Smolder et al.[5,10–24] reported that the membrane porosity could be controlled by the addition of polyvinylpyrrodidone (PVP), salts, or alcohol. Lai et al.[25–27] found that the addition of nonionic surfactants could provoke or inhibit the formation of macrovoids in poly(methyl methacrylate) membranes. In this study, we investigated the effect caused by the addition of nonionic surfactants on the structure of polysulfone membranes and the possible reasons for such an alteration of the membrane structure.

EXPERIMENTAL

Materials

The polysulfone (PSf) used in this study was supplied by AMOCO Performance Products Inc. (Ridgefield,

Correspondence to: R.-C. Ruaan (ruaan@mbox.cycu.edu.tw).
Contract grant sponsor: National Science Council of Taiwan, ROC; contract grant number: NSC 89-2216-E-033-013.

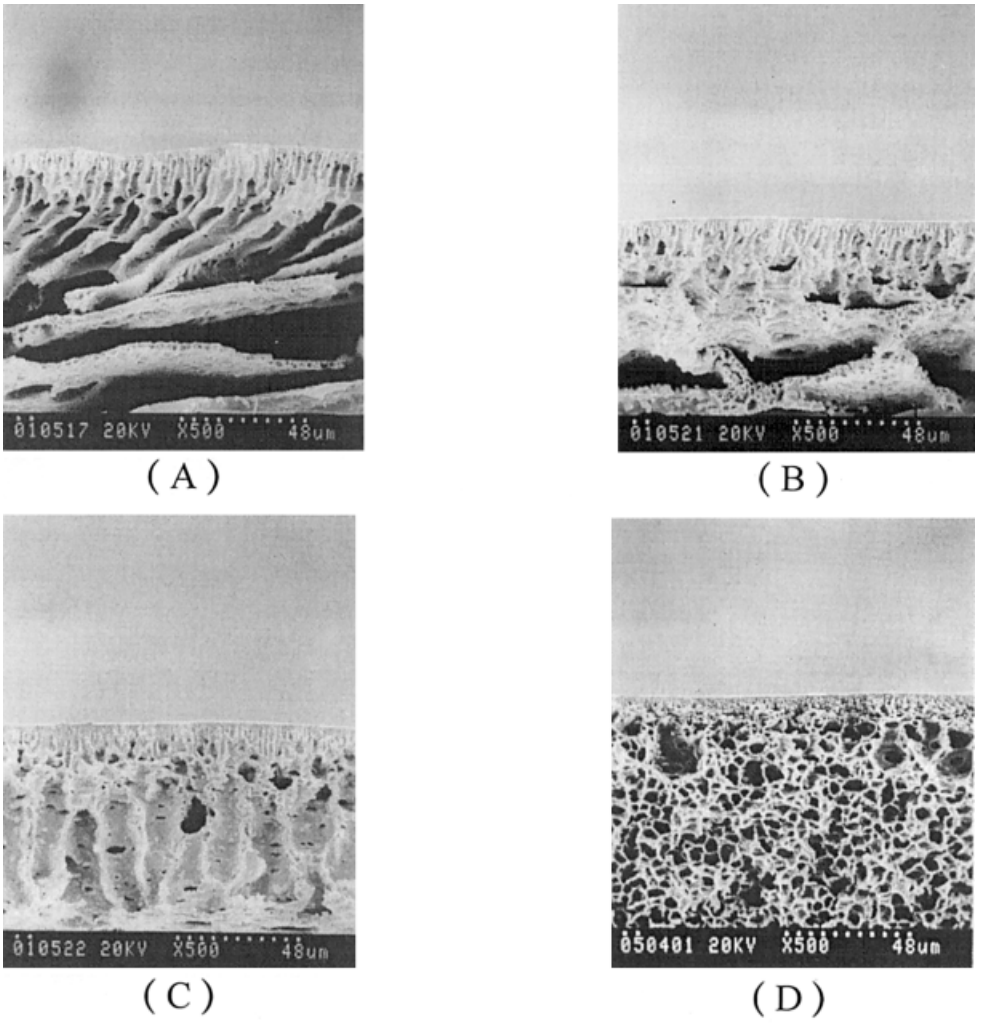

Figure 1 Effect of surfactant in PSf casting solution on membrane morphology; surfactant: Span-80: (A) 0%; (B) 5%; (C) 10%; (D) 15%; coagulant: H_2O; casting temperature: 70°C.

CT) under the trade name of Udel P-3500. The solvent, *N*-methylpyrrolidinone (NMP) was of reagent grade and used without further purification. Distilled water was used as the nonsolvent. The surfactants used in this study were Span-20 (sorbitan monolaurate) and Span-80 (sorbitan monooleate), which were purchased from SHOWA Chemicals Inc. (Tokyo, Japan). The hydrophilic lipophilic balance (HLB) values were 8.6 and 4.3, respectively.

Membrane preparation

The surfactant Span-20 or Span-80 was added to NMP to a concentration of 0–15 wt %. PSf was dissolved in the above solvent mixture to form a 10 wt % casting solution at a predetermined temperature. The degassed casting solution was cast onto a preheated glass plate to a thickness of 300 μm by a preheated Gardner knife. The nascent membrane was immediately immersed into a distilled water coagulation bath at the same temperature and was held at least 1 day (the distilled water was refreshed at least four times). The obtained membranes were peeled off and air-dried completely at ambient temperature.

SEM analysis

The membrane structures were examined by a Hitachi (Model S570) scanning electron microscope (SEM). The membrane samples were fractured in liquid nitrogen and then coated with gold.

Overall porosity

The porosity can be calculated by the following equation:

$$\text{Porosity} = \frac{V_m - V_p}{V_m} \times 100\%$$

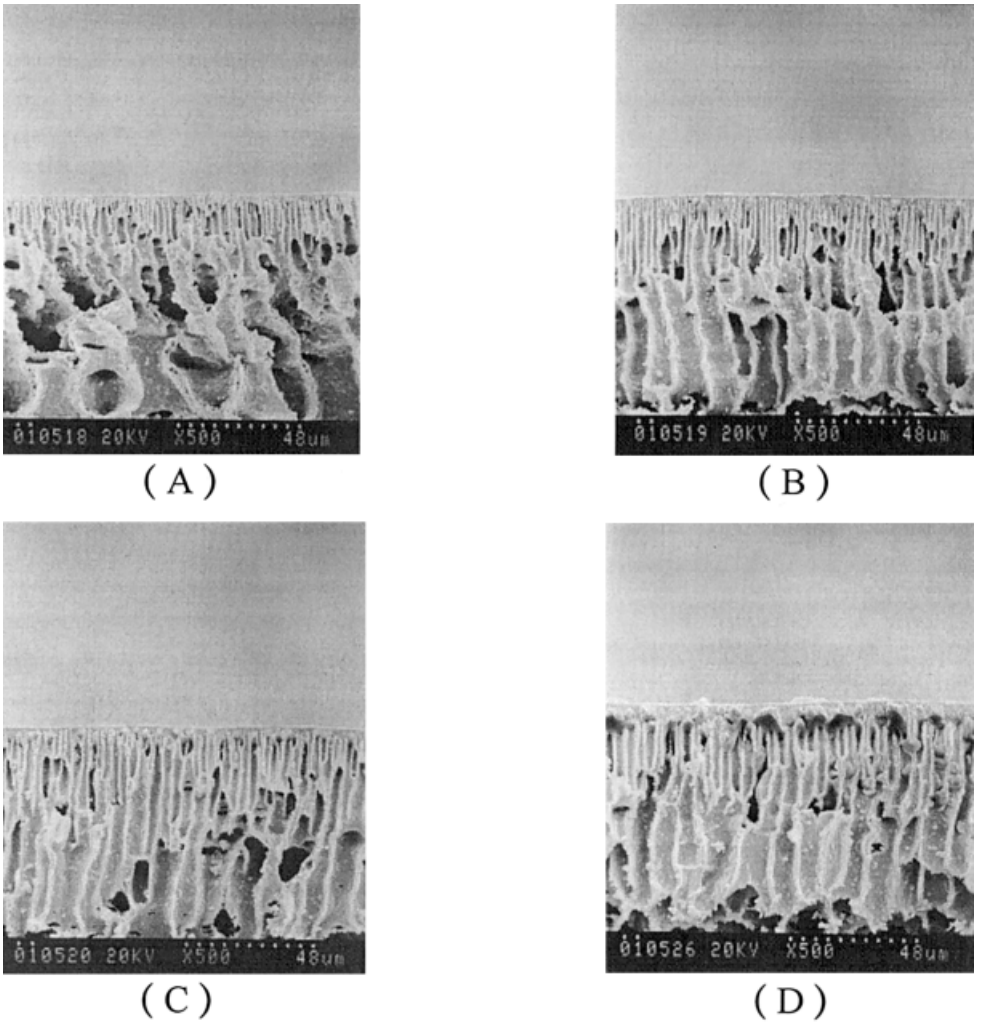

Figure 2 Effect of surfactant in PSf casting solution on membrane morphology; surfactant: Span-20: (A) 5%; (B) 10%; (C) 15%; (D) 20%; coagulant: H_20; casting temperature: 70°C.

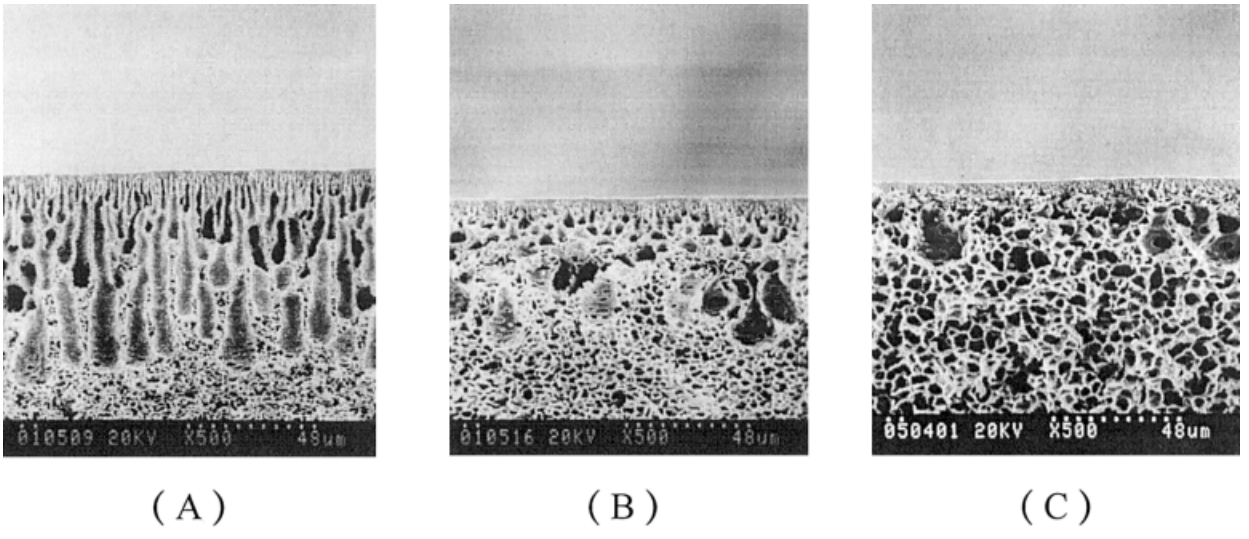

Figure 3 Effect of casting temperature on membrane morphology; temperature: (A) 30°C; (B) 50°C; (C) 70°C; surfactant: 15 wt % Span-80; coagulant: H_2O.

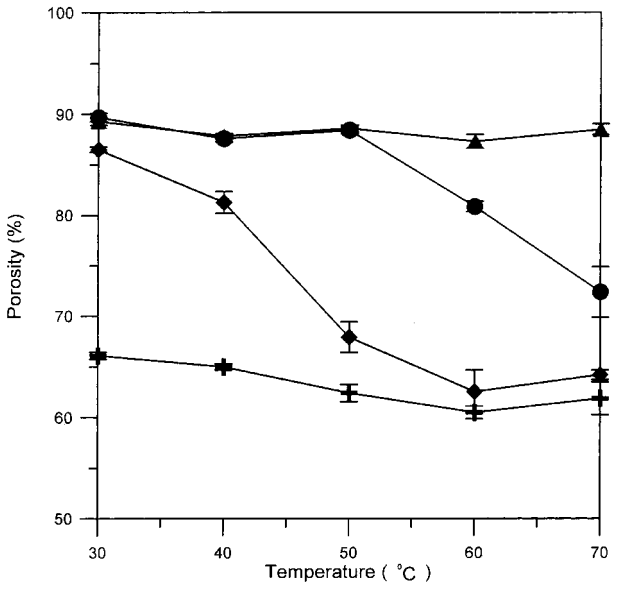

Figure 4 Effect of Span-80 and casting temperature on membrane porosity. Span-80: (▲) 0%; (●) 5%; (◆) 10%; (+) 15%.

where V_m is the bulk volume of the membrane and V_p represents the polymer volume. V_m is obtained by multiplying the membrane area by its thickness. The membrane thickness was measured by a thickness gauge of film (Teclock Corp., Japan). The volume occupied by the polymer (V_P) can be calculated by W_m/ρ_P, where W_m is the weight of the membrane and ρ_P is the density of polymer and has a value of 1.24 g/cm^3 for PSf (measured by Micromeritics, Accupyc Co. Model 1330).

Determination of cloud-point curves

The cloud point was obtained by simple titration. Homogeneous PSf casting solutions of various compositions were prepared and the coagulant, distilled water, was added to each casting solution slowly until the solution became slightly turbid. During titration, the solution was well stirred and kept at a constant temperature. The composition at which permanent turbidity first occurred was called the cloud point, which represents the composition where the phase transition occurred. The cloud-point curve can be interpreted as the envelope of the demixing region.[4] The cloud points were marked on the ternary phase diagram, including only the solvent, nonsolvent, and polymer. The surfactant was treated as the fourth component, which was included in neither the solvent nor the nonsolvent.

Light-transmission experiment

Light-transmission experiments were performed to measure the time period required for on-setting phase separation. The experimental setup and operating procedures were the same as those described in Reuvers.[9]

Viscometry

The viscosity of the PSf casting solution was measured using a Brookfield viscometer (DV-I+; Brookfield En-

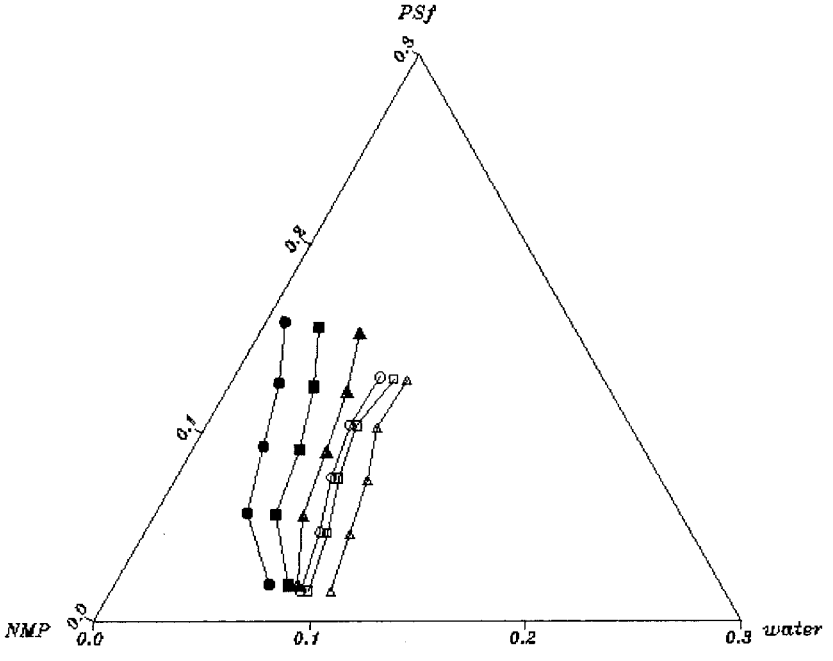

Figure 5 Effect of surfactant and temperature on phase-separated curve of PSf/NMP + 15 wt % Span-80/H_2O: (●) 30°C; (■) 50°C; (▲) 70°C. PSf/NMP/H_2O: (○) 30°C; (□) 50°C; (△) 70°C.

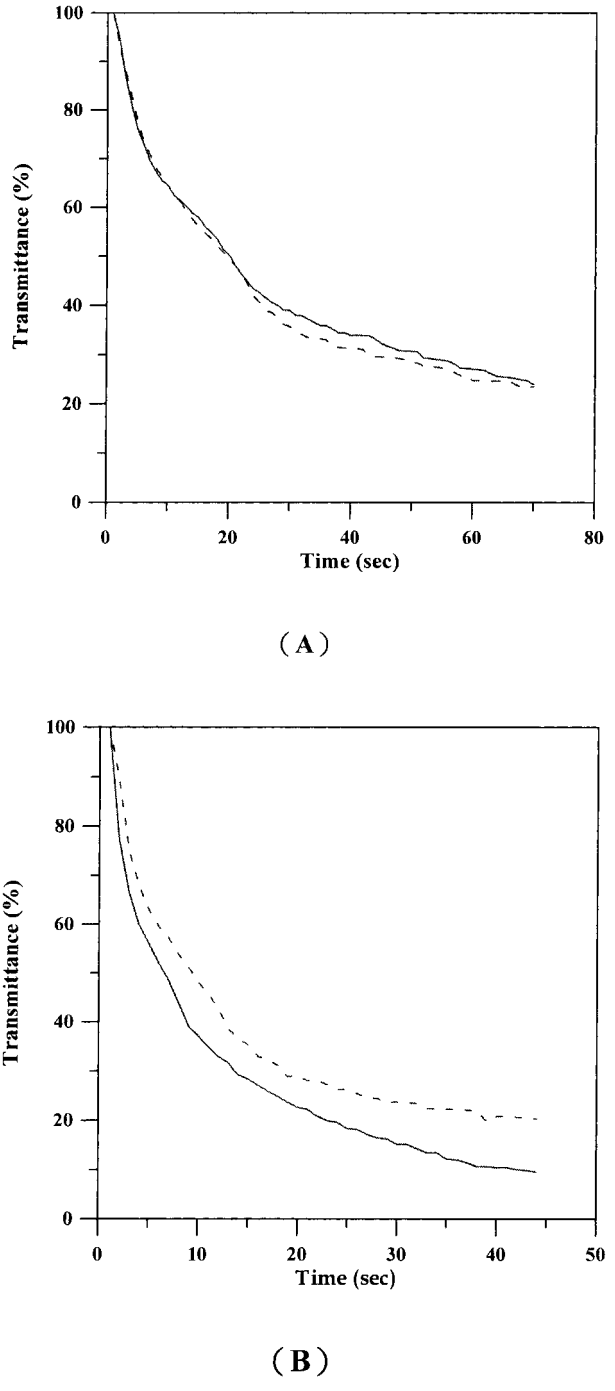

Figure 6 Light-transmission experiments for various conditions: (—) PSf/NMP/H_2O; (–) PSf/NMP + 15% Span-80/H_2O; casting at (A) 30°C and (B) 70°C.

gineering Labs. Inc., Stoughton, MA). The used cell was jacketed by water to maintain a constant temperature.

Penetration experiments

The method used in this study to observe the penetration of water into the casting solution was similar to that described in Strathmann et al.[28] and Wang et al.[11] A drop of the casting solution was placed between two microscope slides and a drop of the coagulant (distilled water), dyed with rhodamine B, was introduced by a syringe. The coagulant penetrated into the casting solution when they were brought into contact. The penetration fronts of water and rhodamine B into the casting solutions were observed and videotaped under an Olympus BHT-M-113D optical microscope. The videotape then was analyzed by an image processing software (Optimas 5.1, Bioscan) to determine the time dependence of the penetration distance of water.

RESULTS

Effect of surfactants

PSf membranes were produced by immersing PSf/NMP nascent membranes in a coagulation tank of distilled water. A highly porous PSf membrane was obtained, as shown in Figure 1(A). When the Span series surfactants were added to the casting solution, the macrovoids were partially inhibited. Figures 1 and 2 show the membrane structure of PSf membranes when various amounts of Span-20 and Span-80 were added. It was obvious that the huge macrovoids were transformed into a slender fingerlike or honeycomb-shape structure after the addition of the surfactants. Span-80 had a stronger influence on the membrane structure than did Span-20. Fifteen percent of added Span-80 was able to completely inhibit the big holes at 70°C, but Span-20 could only turn the huge macrovoids into straight finger-type channels.

Effect of temperature on membrane structure

The fingerlike macrovoids could also be further inhibited by increasing the casting temperature. Figure 3 shows the structure of PSf membranes, of which the casting solution contained 15% Span-80. The membrane had finger-type channels when it was cast at 30°C. The macrovoids changed from a finger to a teardrop shape at 50°C and were almost eliminated at 70°C. It was interesting to find that the temperature had little effect on the structure of the pure PSf membranes but had tremendous influence after the addition of the surfactants. Figure 4 shows the membrane porosity at various temperatures. The porosity of pure PSf remained invariant when cast at different temperatures, but the porosity decreased with the casting temperature when more than 10% Span-80 was added into the casting solution.

Effect of surfactant on coagulating value

Although the increase of the liquid–liquid demixing gap had no obvious relationship with macrovoid for-

TABLE I
Viscosity (cp) of PSf Casting Solution

	Span-80			
Temperature	0%	5%	10%	15%
30°C	75.2–75.6	88.8–89.6	107.0–107.8	132.0–132.6
50°C	50.3–50.5	57.8–58.1	67.0–67.3	80.9–81.1
70°C	34.6–34.7	39.6–39.7	42.5–45.6	53.5–53.6
		Span-20		
	0%	5%	10%	15%
30°C	75.2–75.6	86.0–86.4	109.6–110.8	139.2–139.6
50°C	50.3–50.5	58.8–59.6	68.8–69.6	84.4–85.0
70°C	34.6–34.7	40.6–41.2	47.2–47.6	55.0–55.4

mation, macrovoids were often observed in a system of a low coagulating value, that is, a large demixing gap. We, therefore, compared the cloud-point curves before and after surfactant addition. Figure 5 shows the cloud-point curves at three different casting temperatures. It was found that the addition of the surfactant had little effect on the cloud point at 70°C, but had a stronger effect at lower temperatures. Interestingly, instead of moving away, the cloud-point curve shifted more closely to the polymer–solvent axis with Span-80 addition at 30 and 50°C, which indicated that the effect of macrovoid inhibition by Span-80 was not at all due to the decrease of the coagulating value. On the other hand, the inhibition of macrovoids by elevating the casting temperature might be explained by decrease of the demixing gap. As can be observed from Figure 5, the cloud-point curve moved away from the polymer–solvent axis as the casting temperature increased.

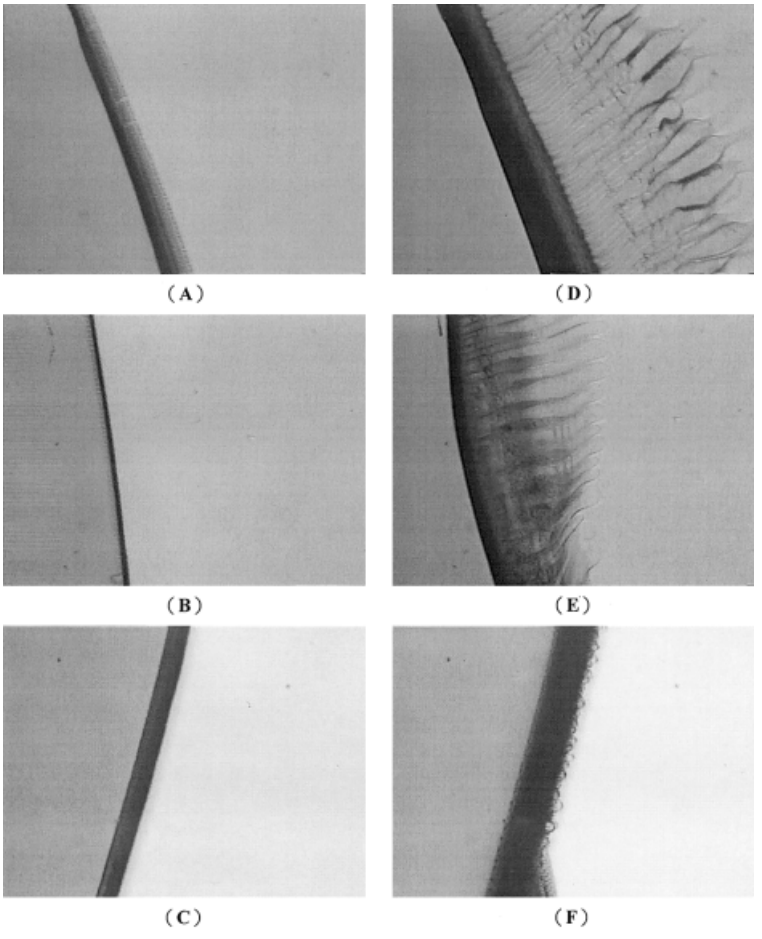

Figure 7 Penetration of coagulant into casting solution (magnification ×50); PSf/NMP system: (A) 0 s; (D) 3 s; PSf/NMP +15 wt % Span-20 system; (B) 0 s; (E) 3 s; PSf/NMP + 15 wt % Span-80 system: (C) 0 s; (F) 3 s.

Effect of surfactants on liquid–liquid demixing rate

Reuvers[9] proposed that the liquid–liquid demixing rate had a strong relation to the membrane structure. They indicated that instantaneous demixing often led to macrovoid formation but delayed demixing often led to a spongelike structure. Figure 6 shows the results of the light-transmission experiments. All the experiments showed instantaneous demixing, with or without Span-80, at 30 or 70°C. It was obvious that the light-transmission experiments could not help us to predict the structures of these membranes.

Viscosity of casting solution

Doi et al.[10] and Cabasso et al.[13,29] suggested that the increase of the viscosity of the casting solution inhibited macrovoid formation. It was believed that the increase in viscosity reduced both the diffusivities of the solvent and the nonsolvent, which resulted in a delayed demixing and subsequently led to a spongelike structure. We measured the viscosity of the PSf/NMP casting solution with or without supplemented surfactants. From Table I, it was found that the addition of surfactants did increase the viscosity of the casting solution and the viscosity increased with the amount of surfactant added. However, the viscosity clearly was not the major factor leading to macrovoid inhibition. The viscosity of the Span-20-containing solution was slightly higher than was the one supplemented with Span-80, but Span-80 had a stronger macrovoid inhibition capability. In addition, the casting solution had a higher viscosity at lower temperatures, but the size of the macrovoids was smaller at higher temperatures.

Penetration test

Strathmann et al.[28] developed a penetration test to observe the membrane-formation process. Using the same technique, we observed the penetration fronts in the beginning and after 3 s of wet inversion, which are illustrated in Figure 7. It was found that the fingertips moved much faster into the surfactant-free and Span-20-containing casting solution, but Span-80 seemed to inhibit the growth of fingerlike macrovoids. Figure 8 shows the dependence of the penetration length on the square root of the contacting time. A linear relation was obtained only when the casting solution contained Span-80 ($R^2 = 0.98$). If we assumed that the penetration front was caused by water diffusion, a water diffusivity of 4.62×10^{-6} cm^2/s could be calculated, which was an order of magnitude smaller than that of the Span-20 one. This value was comparable with that obtained by Barton et al.[30] They measured the moving velocity of the diffusion front of water in a polyethersulfone/DMF casting solution. The estimated water diffusivity was 1.98×10^{-6} cm^2/s when the coagulant contained 80% DMF and the resulting membrane had a spongelike structure. If a similar calculation was performed for the case of a fingerlike membrane structure, water diffusivity similar or higher than pure water diffusivity could be obtained. The above result implied that, at 30°C, the fingerlike structure made from the Span-20-containing casting solution was probably caused by a convective water flow, but that made from Span-80 was by water diffusion. This suggested that the macrovoid inhibition

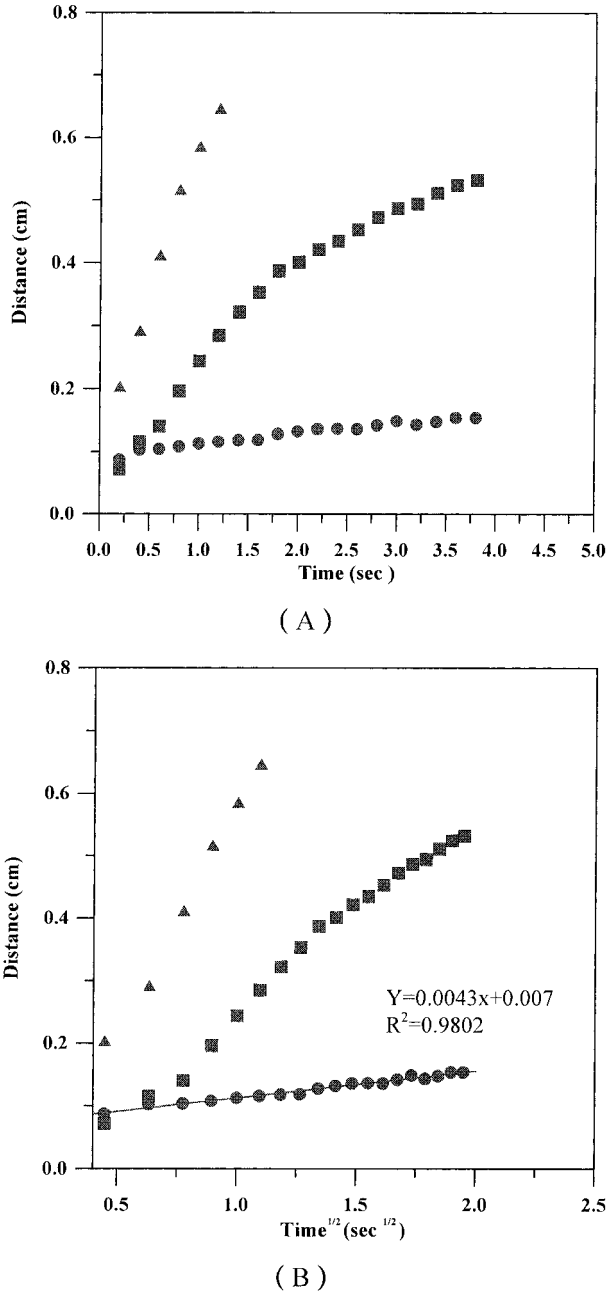

Figure 8 Penetration distance of coagulant versus time: (▲) PSf/NMP/H_2O; (■) PSf/NMP + 15 wt % Span-20/H_2O; (●) PSf/NMP + 15 wt % Span-80/H_2O.

by Span-80 was due to the reduction of the rate of water inflow.

CONCLUSIONS

The addition of Span-80 could effectively inhibit the formation of vast macrovoids. None of the measurements, the position of the cloud-point curve, the change of viscosity, or the light-transmission pattern, could explain the effect caused by Span-80. Only the penetration experiment offered a reasonable explanation. This suggested that the macrovoids were inhibited by the reduction of the water penetration rate. Strathmann et al.[28] suggested that a fingerlike structure was formed when the rate of the nonsolvent inflow was faster than was the rate of the solvent outflow. However, when the rate of the solvent outflow was faster than the rate of the nonsolvent inflow, a spongelike membrane was formed. Conforming to the suggestion from Strathmann et al., the retardation of water inflow by adding Span-80 could effectively inhibit the formation of macrovoids.

The authors wish to sincerely thank the National Science Council of Taiwan, ROC (NSC 89-2216-E-033-013), for the financial support.

References

1. Mulder, M. Basic Principles of Membrane Technology; Kluwer: London, 1991.
2. Altena, F. W.; Smolders, C. A. Macromolecules 1982, 15, 1491.
3. Wijmans, J. G.; Kant, J.; Mulder, M. V.; Smolders, C. A. Polymer 1985, 26, 1539.
4. Lau, W. W. Y.; Guiver, M. D.; Matsuura, T. J Membr Sci 1991, 59, 219.
5. Smolders, C. A.; Reuvers, A. J.; Boom, R. M.; Wienk, I. M. J Membr Sci 1992, 73, 259.
6. Tsay, C. S.; McHugh, A. J. J Polym Sci Part B Polym Phys 1990, 28, 1327.
7. Radovanovic, P.; Thiel, S. W.; Hwang, S. T. J Membr Sci 1992, 65, 213.
8. Radovanovic, P.; Thiel, S. W.; Hwang, S. T. J Membr Sci 1992, 65, 231.
9. Reuvers, A. J. Ph.D. Thesis, Twente University of Technology, The Netherlands, 1987.
10. Doi, S.; Hamanaka, K. Desalination 1991, 80, 167.
11. Wang, D. M.; Lin, F. C.; Chiang, J. C.; Lai, J. Y. J Membr Sci 1998, 141, 1.
12. Kesting, R. E.; Fritzsche, A. K.; Cruse, C. A.; Moore, M. D. J Appl Polym Sci 1990, 40, 1575.
13. Cabasso, I.; Klein, E; Smith, J. K. J Appl Polym Sci 1977, 21, 165.
14. Miao, X.; Sourirajan, S.; Lau, W. W. Y. Sep Sci Technol 1996, 31, 327.
15. Pinnau, I.; Koros, W. J. J Membr Sci 1992, 71, 81.
16. Fritzsche, A. K.; Kesting, R. E.; Murphy, M. K. J Membr Sci 1989, 46, 135.
17. Lai, J. Y.; Lin, F. C.; Wang, C. C.; Wang, D. M. J Membr Sci 1996, 118, 49.
18. Torrestiana-Sanchez, B.; Ortiz-Basurto, R. I.; Brito-De La Fuente, E. J Membr Sci 1999, 152, 19.
19. Wang, D.; Li, K.; Teo, W. K. J Membr Sci 1996, 115, 85.
20. Kim, S. R.; Lee, K. H.; Jhon, M. S. J Membr Sci 1996, 119, 59.
21. Kim, J. H.; Lee, K. H. J Membr Sci 1998, 138, 153.
22. Kang, Y. S.; Kim, H. J.; Kim, U. Y. J Membr Sci 1991, 60, 219.
23. Boom, R. M.; Wienk, I. M.; van den Boomgaard, Th.; Smolders, C. A. J Membr Sci 1992, 73, 277.
24. Wang, D.; Li, K.; Teo, W. K. J Membr Sci 1995, 98, 233.
25. Lai, J. Y.; Lin, F. C.; Wu, T. T.; Wang, D. M. J Membr Sci 1999, 155, 31.
26. Lin, F. C.; Wang, D. M.; Lai, C. L.; Lai, J. Y. J Membr Sci 1997, 123, 281.
27. Wang, D. M.; Lin, F. C.; Wu, T. T.; Lai, J. Y. J Membr Sci 1998, 142, 191.
28. Strathman, H.; Kock, K.; Amar, P.; Baker, R. W. Desalination 1975, 16, 179.
29. Cabasso, I.; Klein, E.; Smith, J. K. J Appl Polym Sci 1976, 20, 2377.
30. Barton, B. F.; Reeve, J. L.; McHugh, A. J. J Polym Sci B Polym Phys 1997, 35, 569.